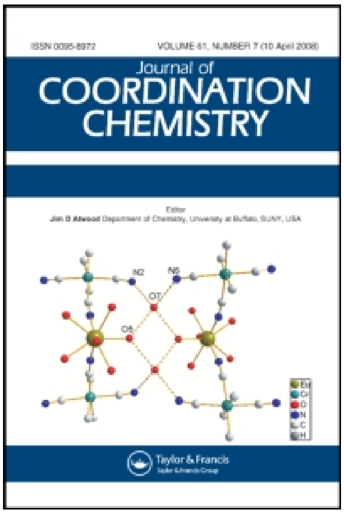

Journal of Coordination Chemistry
Publication details, including instructions for authors and subscription information:
http://www.informaworld.com/smpp/title~content=t713455674

Co-crystallizing coordination compounds

Anders Lennartson[a]
[a] Department of Physics and Chemistry, University of Southern Denmark, DK-5230 Odense M, Denmark

First published on: 20 November 2010

To cite this Article Lennartson, Anders(2010) 'Co-crystallizing coordination compounds', Journal of Coordination Chemistry, 63: 24, 4177 — 4187, First published on: 20 November 2010 (iFirst)
To link to this Article: DOI: 10.1080/00958972.2010.535145
URL: http://dx.doi.org/10.1080/00958972.2010.535145

Journal of Coordination Chemistry
Vol. 63, No. 24, 20 December 2010, 4177–4187

Taylor & Francis
Taylor & Francis Group

Co-crystallizing coordination compounds

ANDERS LENNARTSON*

Department of Physics and Chemistry, University of Southern Denmark,
Campusvej 55, DK-5230 Odense M, Denmark

(*Received 12 August 2010; in final form 13 October 2010*)

Crystallization of an equimolar mixture of 1,10-dimethylphenanthroline (DMP) and manganese(II) chloride from *N*,*N*-dimethylformamide (DMF) has been studied. Rather than a useful route to a well-defined product, it was found that identical solutions could deposit crystals of three different compounds. The most common outcome was the formation of crystals of $[MnCl_2(dmp)(dmf)]$, **1**, or co-crystallization of $[MnCl_2(dmp)(dmf)]$ and $[\{MnCl_2(dmp)\}_2]$. The co-crystals, **2**, were always found to dissolve as crystals of **1** started to grow. Crystals of a third compound, $[MnCl_2(dmp)_2]$, **3**, were also isolated once.

Keywords: Co-crystallization; Manganese; Coordination compounds; Crystallization

1. Introduction

The Cambridge Structural Database [1] contains thousands of structures of two or more different molecules co-crystallizing within the same unit cell. Both organic and coordination compounds frequently co-crystallize with solvent molecules, and there is a vast number of co-crystallizing organic molecules. In comparison, co-crystallization of coordination compounds is far less common. For example, co-crystallization of the two organometallic compounds $[(Cp)_2Y(\mu\text{-C1})_2Li(thf)_2]$ and $[(Cp)_2(Cl)Y(\mu\text{-Cl})Li(thf)_3]$, where Cp is η^5-cyclopentadienyl and thf is tetrahydrofuran, was reported in 1992 [2]. The two molecules differ in the linkage between the two metal centers, and in the number of THF molecules coordinated to Li. The two co-crystallizing organometallic compounds $[Sn(n\text{-Bu})_2(H_2O)_5](CF_3SO_3)_2$ and $[Sn(n\text{-Bu})_2(BPDO\text{-II})(H_2O)_2](CF_3SO_3)_2$, where BPDO-II is 4,4′-dipyridine *N*,*N*′-dioxide, are more different, and differ in the chemical identity of the coordinated ligands [3]. In the case of nickel(II) acetate complexes of the tridentate Schiff-base ligand 2-[(3-methylamino-propylimino)-methyl]-phenol, co-crystallization of dinuclear and trinuclear complexes were reported [4]. Co-crystallizing coordination compounds may have different oxidation states such as the co-crystallizing copper(I)/copper(II) complexes $[Cu^I(H_2CPz_2)(MeCN)_2](ClO_4)$ and $[Cu^{II}(H_2CPz_2)(ClO_4)_2]$, where H_2CPz_2 is *bis*(pyrazol-1-yl)methane, reported in 2005 [5]. Co-crystallizing coordination compounds frequently occur as isomers: two co-crystallizing copper(II) tetrafluoroborate complexes of the potentially tridentate ligand

---

*Email: lennartson@ifk.sdu.dk

Journal of Coordination Chemistry
ISSN 0095-8972 print/ISSN 1029-0389 online
DOI: 10.1080/00958972.2010.535145

bis(2-picolyl)amine have been reported: one of the molecules displays an octahedral coordination geometry, while the other molecule is five-coordinate with one of the pyridyl groups non-coordinated [6]. Chiral cobalt(III) complexes displaying the racemic tetradentate ligand 2,5-diaza-3-methyl-1,6-di(2-pyridyl)hexane and (*S*)-alanine crystallize with four diastereomers in the unit cell [7, 8]. Two geometrical isomers may also appear as disorder in the crystal structure [9]. We have previously reported co-crystallization of square pyramidal *cis*- and *trans*-pyridine-*bis*(benzoylacetonato)-copper(II) [10], a rare example of co-crystallization of two well-ordered geometrical isomers displaying the same coordination [11, 12]. In this article, we report the co-crystallization of a mononuclear and a dinuclear manganese(II) complex.

2. Experimental

2.1. *Crystallization*

Manganese(II) chloride (Aldrich) and neocuproine hemihydrate (Aldrich) were used as received. Manganese(II) chloride (0.12 g, 1 mmol) and neocuproine hemihydrate (0.21 g, 1 mmol) were dissolved in *N*,*N*-dimethylformamide (1.5 mL). Yellow crystals formed overnight. Yield (**1**): 0.30 g (74%). Yield (**2**): 0.25 g (67%). IR (**1**, KBr): 3380 (s), 3294(s), 3017(w), 2921(w), 1655(s), 1618(w), 1591(m), 1553(s), 1500(m), 1436(m), 1389(m), 1293(m), 1250(m), 1218(m), 1149(s), 1117(s), 1026(m), 988(w), 930(w), 770(s), 732(s), 679(s), 647(s), and 551(s) cm^{-1}.

2.2. *Crystallography*

Crystals of **1**–**3** were carefully selected using a microscope at low temperature [13]. Data were recorded at 100 K using a Rigaku R-AXIS IIc area detector with graphite monochromated Mo-Kα radiation ($\lambda = 0.71073$ Å) from a Rigaku RU-H3R rotating anode, operating at 50 kV and 90 mA; 90 oscillation photos with a rotation angle of 2° were collected. Data were processed using the CrystalClear software package [14], and an empirical absorption correction was applied using the REQAB program. The structures were solved using the program SIR-92 [15] and refined using full-matrix least squares calculations on F^2 using the SHELXL-97 program [16]. All non-hydrogen atoms were refined anisotropically, and hydrogens were included in calculated positions and refined using a riding model. Figures were drawn using ORTEP3 [17] for Windows or Pluton [18, 19]. SIR-92, SHELXL-97, and ORTEP3 were enclosed in the WinGX-software package [20]. Crystal and refinement data are given in table 1.

3. Results and discussion

Crystallization of an equimolar mixture of 1,10-dimethylphenanthroline (DMP, neocuproine) and anhydrous manganese(II) chloride from *N*,*N*-dimethylformamide (DMF) under apparently identical conditions may have at least three different outcomes. The compound [$MnCl_2$(dmp)(dmf)], **1** (scheme 1, figure 1, and table 2) may

Table 1. Crystal and refinement data for **1**–**3**.

Parameter	**1**	**2**	**3**
Empirical formula	$MnC_{17}H_{19}Cl_2N_3O$	$Mn_2C_{31}H_{31}Cl_4N_5O$	$MnC_{28}H_{24}Cl_2N_4$
M	407.19	741.29	542.35
Temperature (K)	100(2)	100(2)	100(2)
Crystal system	Triclinic	Triclinic	Monoclinic
Space group	$P\bar{1}$	$P\bar{1}$	$C2/c$
Unit cell dimensions (Å, °)			
a	8.4348(7)	9.437(2)	16.585(4)
b	8.7900(10)	13.407(4)	9.9209(19)
c	12.9814(10)	13.774(3)	15.260(3)
α	79.599(18)	107.527(9)	90.00
β	74.683(16)	95.323(3)	109.958(7)
γ	79.326(16)	103.504(7)	90.00
Volume (Å^3), Z	903.38(17), 2	1590.7(7), 1	2360.1(9), 4
Calculated density (g cm^{-3})	1.497	1.548	1.526
μ(Mo-Kα) mm^{-1}	1.035	1.164	0.812
Crystal size (mm^3)	0.3 × 0.3 × 0.3	0.2 × 0.1 × 0.1	0.3 × 0.2 × 0.2
θ range for data collection (°)	3.16–25.00	1.57–25.00	3.03–25.00
Reflections collected	5607	11066	7000
Unique reflections	2860 [R(int) = 0.0314]	5617 [R(int) = 0.0375]	2021 [R(int) = 0.0280]
Number of parameters	225	398	161
Goodness-of-fit on F^2	1.031	1.066	1.050
Final			
$R_1(F)^a(I > 2\sigma(I))/wR_2(F^2)^b$	$R_1 = 0.0444$, $wR_2 = 0.1125$	$R_1 = 0.0254$, $wR_2 = 0.0683$	$R_1 = 0.0219$, $wR_2 = 0.0589$
$R_1{}^a/wR_2(F^2)^b$ (all data)	$R_1 = 0.0463$, $wR_2 = 0.1140$	$R_1 = 0.0284$, $wR_2 = 0.0704$	$R_1 = 0.0242$, $wR_2 = 0.0600$

$^aR_1(F) = \Sigma(\|F_o| - |F_c\|)/\Sigma|F_o|$; $^bwR_2(F^2) = \{\Sigma[w(F_o^2 - F_c^2)^2]/\Sigma[w(F_o^2)^2]\}^{1/2}$.

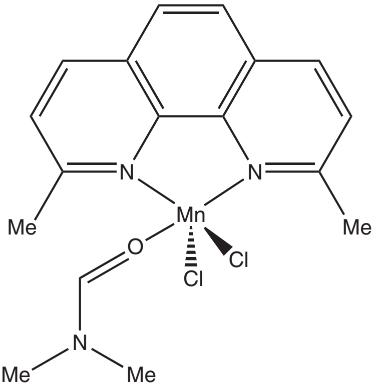

Scheme 1. Molecular constitution of **1**.

form as yellow crystal blocks overnight. The central Mn in **1** is five coordinate, with a coordination geometry best described as highly distorted trigonal bipyramidal. The bidentate dmp spans one equatorial position and one apical position, with the other apical position being occupied by DMF. Two chlorides complete the coordination sphere. The crystal structure of **1** is built up by stacks parallel to the crystallographic *a*-axis (figure 2). There are indications of face-to-face π–π interactions within

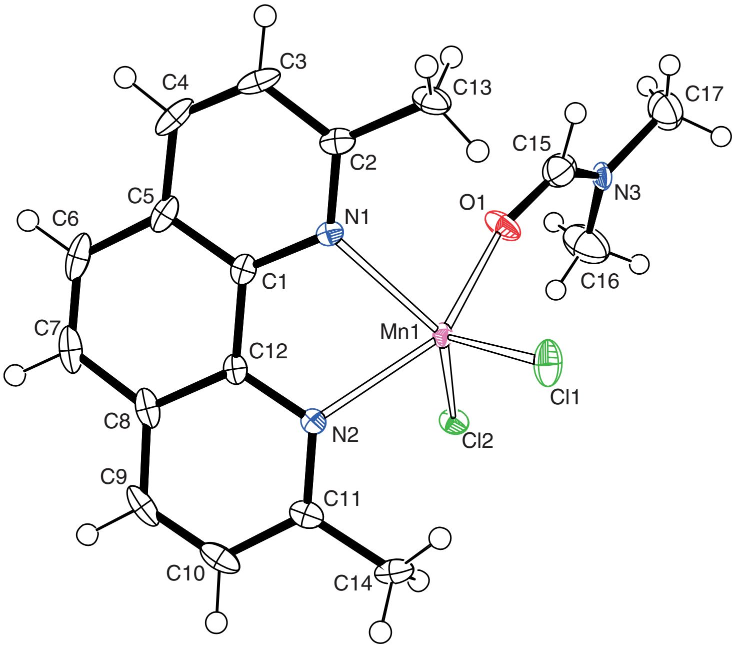

Figure 1. Molecular structure of **1** displaying the crystallographic numbering scheme. Displacement ellipsoids are drawn at the 50% probability level and hydrogens are included as spheres of arbitrary radii.

Table 2. Selected bond distances (Å) and angles (°) for **1**.

Mn(1)–N(1)	2.271(3)
Mn(1)–N(2)	2.270(3)
Mn(1)–O(1)	2.136(2)
Mn(1)–Cl(1)	2.3557(9)
Mn(1)–Cl(2)	2.4379(8)
O(1)–Mn(1)–N(2)	148.34(10)
O(1)–Mn(1)–N(1)	87.30(9)
N(2)–Mn(1)–N(1)	73.27(9)
O(1)–Mn(1)–Cl(1)	104.06(7)
N(2)–Mn(1)–Cl(1)	105.65(7)
N(1)–Mn(1)–Cl(1)	108.20(7)
O(1)–Mn(1)–Cl(2)	88.35(6)
N(2)–Mn(1)–Cl(2)	85.63(6)
N(1)–Mn(1)–Cl(2)	130.03(7)
Cl(1)–Mn(1)–Cl(2)	121.10(4)

these stacks. The N1–C1–C2–C3–C4–C5 and C1–C5–C6–C7–C8–C12 rings are approximately coplanar with the N1^{i}–C1^{i}–C2^{i}–C3^{i}–C4^{i}–C5^{i} and C1^{i}–C5^{i}–C6^{i}–C7^{i}–C8^{i}–C12^{i} rings (symmetry code: (i) $1-x$, $1-y$, $2-z$). The shortest C–C distance, 3.371(4) Å, is between C1 and C6^{i}. At the other face of the dmp ligand, the N1–C1–C2–C3–C4–C5 and C1–C5–C6–C7–C8–C12 rings are approximately coplanar with the N2^{ii}–C8^{ii}–C9^{ii}–C10^{ii}–C11^{ii}–C12^{ii} and C1^{ii}–C5^{ii}–C6^{ii}–C7^{ii}–C8^{ii}–C12^{ii} rings (symmetry code: (ii) $-x$, $1-y$, $2-z$), the shortest C–C-distance, C1–C10^{ii}, being 3.315(4) Å.

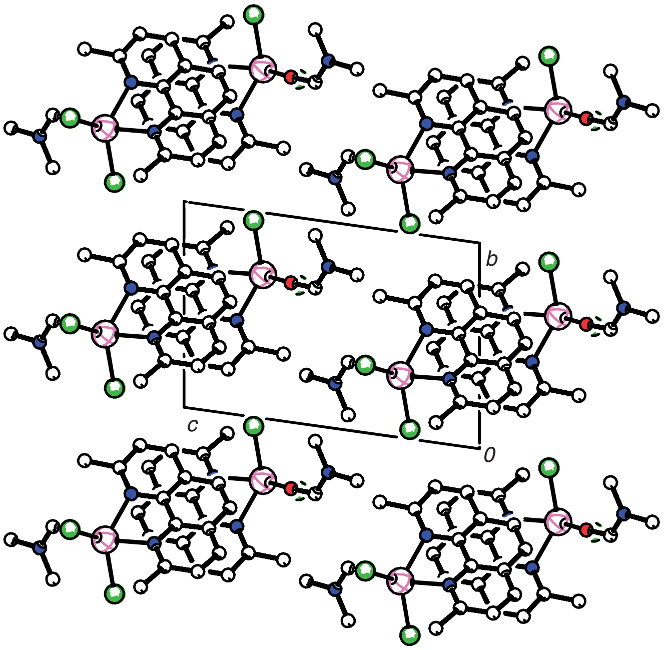

Figure 2. The crystal structure of **1** is built up by stacks parallel to the crystallographic *a*-axis. The stacks are held together through π–π stacking. All hydrogens are omitted for clarity.

The structure is further stabilized by CH–Cl interactions, the shortest H–Cl distance being $H1–Cl1^{iii}$ (symmetry code: (iii) $1-x$, $1-y$, $1-z$), which is 2.84(4) Å. Crystals of **1** are air-sensitive and they readily lose DMF when removed from the mother liquor.

Frequently, however, crystallization afforded thin light yellow needles of [$MnCl_2$(dmp)(dmf)] [{$MnCl_2$(dmp)}$_2$], **2**. The two compounds **1** and **2** are easily distinguished visually, and crystals of **2** form more rapidly than do crystals of **1**. Samples of **2** were always found to transform into **1** within hours or days. Crystals of **1** nucleate separately from **2**, and do not grow form previously formed crystals of **2**, but once **1** starts to crystallize, remaining crystals of **2** dissolve. Addition of crystals of **1** to crystals of **2** in the mother liquor was found to induce transformation, and the two phases cannot coexist in the mother liquor for any extended period of time. Formation of crystals of **2** after crystals of **1** has so far not been observed, indicating that immediate seeding with **1** may suppress the crystallization of **2**. The calculated density of **2** is $1.548\,g\,cm^{-3}$ compared to $1.497\,g\,cm^{-3}$ for **1**, and this would perhaps indicate a higher stability of **2** compared to **1** [21]. The driving force for the transformation is probably a higher solubility of **2** in DMF compared to **1**. This is supported by the fact that yields of **2** were always lower than the yields of **1**.

The [$MnCl_2$(dmp)(dmf)] molecule in **2** (figure 3 and table 3) displays the same arrangement of ligands around the central Mn, but deviates less from a regular trigonal bipyramidal coordination geometry than does the corresponding molecule in **1**. In **2**, [$MnCl_2$(dmp)(dmf)] co-crystallizes with a dinuclear complex, [{$MnCl_2$(dmp)}$_2$] (scheme 2, figure 4, and table 3). This molecule is still five-coordinate, but Mn1 does not coordinate DMF. Instead, one chloride acts as a bridging ligand and the resulting

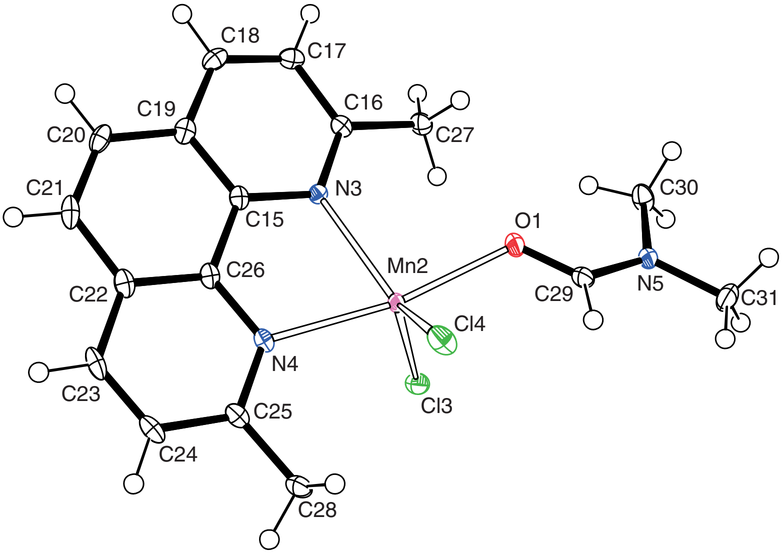

Figure 3. Molecular structure of [$MnCl_2$(dmp)(dmf)] in **2** displaying the crystallographic numbering scheme. Displacement ellipsoids are drawn at the 50% probability level and hydrogens are included as spheres of arbitrary radii.

Table 3. Selected bond distances (Å) and angles (°) for **2**.

Mn(1)–N(1)	2.2286(13)
Mn(1)–N(2)	2.2459(13)
Mn(1)–Cl(1)	2.3350(5)
$Mn(1)^{vi}$–Cl(2)	2.5108(8)
Mn(1)–Cl(2)	2.5216(7)
Mn(2)–N(3)	2.2630(14)
Mn(2)–N(4)	2.2850(13)
Mn(2)–O(1)	2.1768(11)
Mn(2)–Cl(3)	2.3852(6)
Mn(2)–Cl(4)	2.4054(7)
N(1)–Mn(1)–N(2)	74.41(5)
N(1)–Mn(1)–Cl(1)	115.85(4)
N(2)–Mn(1)–Cl(1)	110.31(4)
N(1)–Mn(1)–$Cl(2)^{vi}$	91.13(4)
N(2)–Mn(1)–$Cl(2)^{vi}$	145.13(3)
Cl(1)–Mn(1)–$Cl(2)^{vi}$	104.562(19)
N(1)–Mn(1)–Cl(2)	130.42(3)
N(2)–Mn(1)–Cl(2)	83.35(3)
Cl(1)–Mn(1)–Cl(2)	113.32(2)
$Cl(2)^{vi}$–Mn(1)–Cl(2)	82.507(19)
O(1)–Mn(2)–N(3)	97.89(4)
O(1)–Mn(2)–N(4)	167.79(4)
N(3)–Mn(2)–N(4)	74.15(5)
O(1)–Mn(2)–Cl(3)	91.19(4)
N(3)–Mn(2)–Cl(3)	112.11(3)
N(4)–Mn(2)–Cl(3)	100.35(4)
O(1)–Mn(2)–Cl(4)	87.50(4)
N(3)–Mn(2)–Cl(4)	123.28(4)
N(4)–Mn(2)–Cl(4)	89.27(4)
Cl(3)–Mn(2)–Cl(4)	124.24(2)
C(29)–O(1)–Mn(2)	125.52(10)

Symmetry code: (vi) $1 - x, 1 - y, 2 - z$.

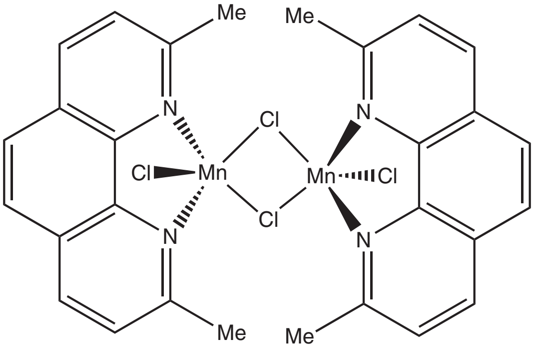

Scheme 2. Molecular constitution of [{$MnCl_2$(dmp)}$_2$] in **2**.

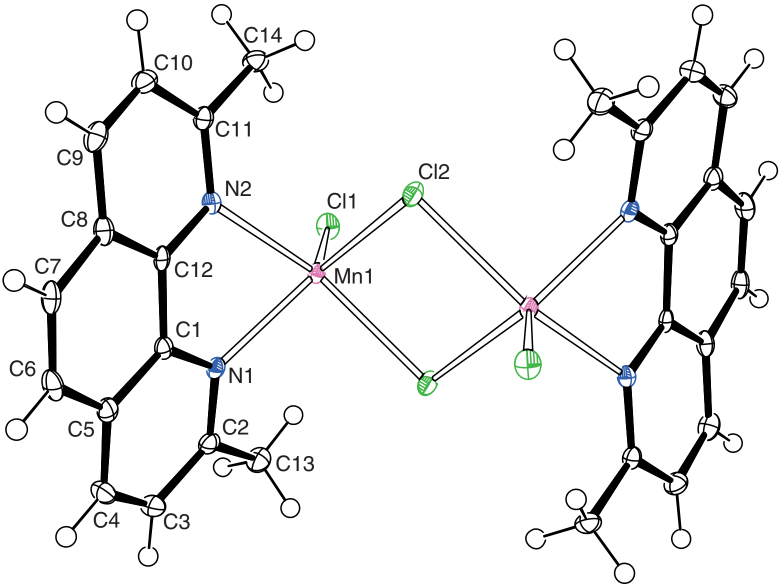

Figure 4. Molecular structure of [{$MnCl_2$(dmp)}$_2$] in **2** displaying the crystallographic numbering scheme. Displacement ellipsoids are drawn at the 50% probability level and hydrogens are included as spheres of arbitrary radii.

dinuclear complex is located at an inversion center. The coordination geometry around Mn1 deviates considerably from both trigonal bipyramidal and square pyramidal, in contrast to the corresponding phenanthroline complex, which displays a coordination geometry close to square pyramidal [22]. There are two sets of short interactions between two molecules in the asymmetric unit. These involve the non-bridging chloride of [{$MnCl_2$(dmp)}$_2$] and the two methyl groups in DMF of [$MnCl_2$(dmp)(dmf)]. The H30C–Cl1 and H31B–Cl1 distances are 2.74 and 2.93 Å, respectively. There are other H–Cl interactions in **2**: H31A–Cl4^{iv} and H14C–Cl3^{v} (2.73 and 2.83 Å, respectively;

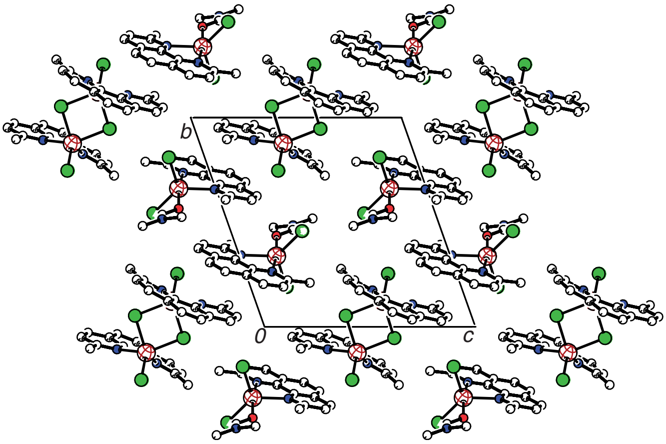

Figure 5. The $[MnCl_2(dmp)(dmf)]$ and $[\{MnCl_2(dmp)\}_2]$ molecules in **2** form discrete stacks parallel to the crystallographic *a*-axis. All hydrogens are omitted for clarity.

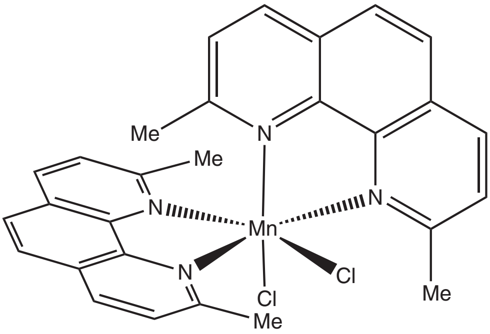

Scheme 3. Molecular constitution of **3**.

symmetry codes: (iv) $2-x$, $1-y$, $1-z$; (v) x, $1+y$, $1+z$). Viewed along the crystallographic *a*-axis (figure 5), the structure is composed of stacks of $[MnCl_2(dmp)(dmf)]$ and $[\{MnCl_2(dmp)\}_2]$ molecules, respectively. Like **1**, crystals of **2** decompose when isolated from the mother liquor.

No crystals of pure $[\{MnCl_2(dmp)\}_2]$ were ever observed. However, during one crystallization, dark yellow needles visually different from the crystals of **1** and **2** were formed. Single-crystal X-ray diffraction showed the crystals to be $[MnCl_2(dmp)_2]$, **3** (scheme 3, figure 6, and table 4). The coordination geometry around Mn in **3** is best described as distorted trigonal prismatic with the molecule situated at a crystallographic two-fold axis. As a result of this coordination geometry, the two dmp-ligands are almost coplanar, which results in intramolecular face-to-face π–π interactions: the shortest C–C distance, 3.180(2) Å, being C1–C11^{vii} (symmetry code: (vii) $1-x$, y, $1/2-z$). This stands in contrast to the molecular structure of the corresponding

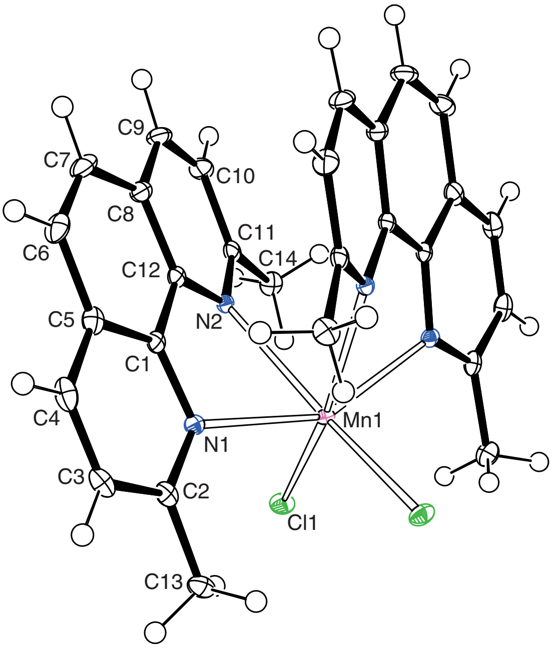

Figure 6. Molecular structure of **3** displaying the crystallographic numbering scheme. Displacement ellipsoids are drawn at the 50% probability level and hydrogens are included as spheres of arbitrary radii.

Table 4. Selected bond distances (Å) and angles (°) for **3**.

Mn(1)–N(1)	2.3117(11)
Mn(1)–N(2)	2.4567(11)
Mn(1)–Cl(1)	2.4441(5)
N(1)–Mn(1)–N(1)^{xi}	150.53(6)
N(1)–Mn(1)–Cl(1)	98.27(3)
N(1)–Mn(1)–Cl(1)^{xi}	99.66(3)
Cl(1)–Mn(1)–Cl(1)^{xi}	104.47(2)
N(1)–Mn(1)–N(2)^{xi}	87.14(4)
Cl(1)–Mn(1)–N(2)^{xi}	161.94(3)
N(1)–Mn(1)–N(2)	69.17(4)
Cl(1)–Mn(1)–N(2)	91.47(3)
N(2)^{xi}–Mn(1)–N(2)	74.27(5)

Symmetry code: (xi) $1 - x$, y, $1/2 - z$.

phenanthroline complex, which displays octahedral coordination geometry [23]. CH–Cl interactions in **3** give rise to chains extended parallel to the crystallographic *b*-axis. The H9–Cl1^{viii} (symmetry code: (viii) x, $1+y$, z) distance is 2.82 Å. In addition, H9^{vii} interacts with Cl1^{ix} (symmetry code: (ix) $1-x$, $1+y$, $1/2-z$), and as a result each molecule is involved in four interactions of this type. A second set of interactions, H14C–Cl1^{x} (symmetry code: (x) $1/2-x$, $1/2+y$, $1/2-z$) of 2.88 Å connects the chains into layers on the (−4 0 4) set of planes. As seen from figure 7, stacks are also formed parallel to the crystallographic *c*-axis.

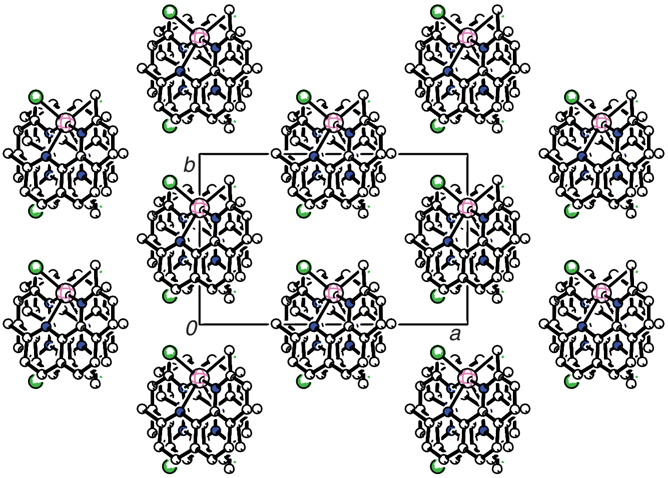

Figure 7. Stacks formed parallel to the crystallographic *c*-axis in the crystal structure of **3**. All hydrogens are omitted for clarity.

We have previously shown how crystallization of 10-nitro-phenantren-9-yl phenyl sulphide [24], dichloro-di(2,4-lutidine)zinc(II) [25] and diindenyl-di(3-picoline)zinc(II) [26] may lead to concomitant polymorphism [27]. Synthesis always gave the same chemical compound, but upon crystallization these stereochemically labile, chiral compounds could give rise to chiral crystals, racemic crystals or mixtures of the two phases. Especially in the case of dichloro-di(2,4-lutidine)zinc(II) the outcome was completely unpredictable. The innocent-looking $MnCl_2$–DMP–DMF system presents another type of anomaly: rather than forming a well-defined and predictable product, identical solutions may deposit crystals of (at least) three different compounds, one of which is a comparably rare example of co-crystallizing coordination compounds. So far, we have no method for reproducible preparation of either **1**, **2**, or **3**.

Supporting material

CCDC 781641 (**1**), 781642 (**2**), and 781643 (**3**) contain the supplementary crystallographic data for this article. These data can be obtained free of charge from The Cambridge Crystallographic Data Centre *via* www.ccdc.cam.ac.uk/data_request/cif. Supplementary material associated with this article can be found in the online version.

References

[1] F.H. Allen. *Acta Cryst*., **B58**, 380 (2002).
[2] W.J. Evans, T.J. Boyle, J.W. Ziller. *Inorg. Chem*., **31**, 1120 (1992).
[3] V. Chandrasekhar, P. Singh. *Organometallics*, **28**, 4974 (2009).
[4] P. Mukherjee, M.G.B. Drew, C.J. Gomez-Garcia, A. Ghosh. *Inorg. Chem*., **48**, 4817 (2009).
[5] C.-C. Chou, C.-C. Su, H.-L. Tsai, K.-H. Lii. *Inorg. Chem*., **44**, 628 (2005).

[6] M. Palaniandavar, R.J. Butcher, A.W. Addison. *Inorg. Chem.*, **35**, 467 (1996).
[7] M.W. Mulqi, P.A. Williams, F.S. Stephens, R.S. Vagg. *Inorg. Chim. Acta*, **88**, 183 (1984).
[8] P. Jones, R.S. Vagg, P.A. Williams. *Inorg. Chem.*, **23**, 4110 (1984).
[9] R.C. Holz, L.C. Thompson. *Inorg. Chem.*, **32**, 5251 (1993).
[10] A. Lennartson, M. Håkansson, S. Jagner. *New J. Chem.*, **31**, 344 (2007).
[11] R.G. Hazell. *Acta Chem. Scand.*, **22**, 2171 (1968).
[12] W. Purcell, S.S. Basson, J.G. Leipoldt, A. Roodt, H. Preston. *Inorg. Chim. Acta*, **234**, 153 (1995).
[13] M. Håkansson. *Inorg. Synth.*, **32**, 222 (1998).
[14] CrystalClear 1.3 (c)1998–2001 Rigaku.
[15] A. Altomare, G. Cascarano, C. Giacovazzo, A. Gualardi. *J. Appl. Cryst.*, **26**, 343 (1993).
[16] G.M. Sheldrick. *Acta Cryst.*, **A64**, 112 (2008).
[17] L.J. Farrugia. *J. Appl. Cryst.*, **30**, 565 (1997).
[18] A.L. Spek. *Acta Cryst.*, **A46**, C34 (1990).
[19] A.L. Spek. *PLATON. A Multipurpose Crystallographic Tool*, Utrecht University, Utrecht, The Netherlands (2002).
[20] L.J. Farrugia. *J. Appl. Cryst.*, **32**, 837 (1999).
[21] A. Burger, R. Ramberger. *Mikrochimica Acta*, **2**, 259 (1979).
[22] X.-Y. Hou, J.-J. Wang, X. Wang, D.-S. Li, J.-W. Wang. *Z. Kristallogr. – New Cryst. Struct.*, **222**, 57 (2007).
[23] T.J. Malinowski, V.C. Kravtsov, Y.A. Simonov, J. Lipkowski, O.A. Bologa. *J. Coord. Chem.*, **37**, 187 (1996).
[24] A. Lennartson, T. Wiklund, M. Håkansson. *CrystEngComm.*, **9**, 856 (2007).
[25] A. Lennartson, S. Olsson, J. Sundberg, M. Håkansson. *Inorg. Chim. Acta*, **363**, 257 (2009).
[26] A. Lennartson, S. Olsson, J. Sundberg, M. Håkansson. *Angew. Chem. Int. Ed.*, **48**, 3137 (2009).
[27] J. Bernstein, R.J. Davey, J.-O. Henck. *Angew. Chem., Int. Ed.*, **38**, 3441 (1999).